A quantum walk in phase space with resonator-assisted double quantum dots*

Zhi-Hao Bian(边志浩), Hao Qin(秦豪), Xiang Zhan(詹翔), Jian Li(李剑), and Peng Xue(薛鹏)†

Department of Physics, Southeast University, Nanjing 211189, *China*

(Received 11 August 2015; revised manuscript received 4 October 2015; published online 20 December 2015)

We implement a quantum walk in phase space with a new mechanism based on the superconducting resonator-assisted double quantum dots. By analyzing the hybrid system, we obtain the necessary factors implementing a quantum walk in phase space: the walker, coin, coin flipping and conditional phase shift. The coin flipping is implemented by adding a driving field to the resonator. The interaction between the quantum dots and resonator is used to implement conditional phase shift. Furthermore, we show that with different driving fields the quantum walk in phase space exhibits a ballistic behavior over 25 steps and numerically analyze the factors influencing the spreading of the walker in phase space.

Keywords: quantum walks, double quantum dots

PACS: 03.67.Ac, 42.50.Pq, 74.50.+r **DOI:** 10.1088/1674-1056/25/2/020307

1. Introduction

Quantum walk (QW)[1] is appealing as an intuitive model in quantum algorithms[2–4] and quantum simulations,[5–8] because it exponentially speeds up the hitting time in glued tree graphs. Furthermore, QW offers a quadratic gain over classical algorithms on account of the diffusion spread (standard deviation), which is proportional to elapsed time t, rather than $\sqrt{t}$ for the classical random walk (RW).[9–12] Thus, the conception of physical implementation of QW has become important and attracts more and more attention. Although QWs have been realized experimentally in different systems such as trapped ions,[13–15] photons,[16–28] nuclear magnetic resonance,[29,30] etc., the solid state system is attractive because of its stability and expected scalability.

Recently, quantum computing with quantum dots has made huge progress,[31–38,40–42] and the technique for coupling electrons associated with a semiconductor double-dot molecule to a microwave stripline resonator has become more and more matured. Here we make use of this technology and propose the implementation of a one-dimensional QW in phase space (PS) with superconducting resonator-assisted quantum double-dot. The walker is presented by a coplanar transmission line resonator with a single mode, and a two-level system — one electron shared by double dots via tunneling serves as the quantum coin.

In our scheme the QW is executed with indirect flipping of the coin via directly driving the resonator and allows controllable decoherence over circles in PS for observing the transition between QW and RW.[11,39,43] In the next section, we give a brief introduction of the QW in PS. In Section 3, we implement QW via realizing the walker, coin, coin flipping and conditional phase shift. In addition to the numerical analysis under the different driving fields, we observe the ballistic behavior of QW in PS and the QW–RW transmission with the influence of decoherence introduced by the shift operation in the position space.

2. Brief introduction of QW in PS

Like for the QW on a line in position space in which the walker moves towards the left or right based on the coin state, for QW on a circle in PS, the walker rotates either clockwise or counter-clockwise along the circle in PS by the same amount, say an angle $\Delta\theta$, with the strictly random choice of $\pm\Delta\theta$ through the impulse, which is applied by a harmonic oscillator.

In an ideal QW on a circle, the coin is replaced by a two-level system with internal states $|0\rangle$ and $|1\rangle$. Here we introduce the finite-dimensional orthogonal phase state representation[44]

$$|\theta_k = \frac{2\pi k}{d}\rangle = \frac{1}{\sqrt{d}}\sum_{n}^{d-1} \mathrm{e}^{\mathrm{i}n\theta_k}|n\rangle, k \in Z, \tag{1}$$

where $|n\rangle$ is the Fock state. If the step size $\Delta\theta = 2\pi/d$, $d \in N$, then the walker always remains on the circle with angular lattice spacing $\Delta\theta$. The walker walks in PS with a state $|\theta_k\rangle$ which can be decomposed into the phase states. Introduce the rotation operator $\hat{R}_m = \mathrm{e}^{\mathrm{i}n\theta_m}$, $m \in Z$, and we will have $\hat{R}_m|\theta_k\rangle = |\theta_{k+m}\rangle$. We choose the Hadamard operator

$$H = \frac{1}{\sqrt{2}}\begin{pmatrix} 1 & 1 \\ 1 & -1 \end{pmatrix} \tag{2}$$

as the coin flipping operator and the unitary operation of one

*Project supported by the National Natural Science Foundation of China (Grant No. 11474049) and CAST Innovation Fund.

†Corresponding author. E-mail: gnep.eux@gmail.com

© 2016 Chinese Physical Society and IOP Publishing Ltd

step of the QW in PS is given by

$$E = \mathrm{e}^{in\sigma_z \Delta\theta} \tag{3}$$

with the number operator on the walker state $n = a^\dagger a$, $a^\dagger$ and a are the creation and annihilation operators, respectively, and $\sigma_z = \begin{pmatrix} 1 & 0 \\ 0 & -1 \end{pmatrix}$ is one of the Pauli operators on the coin.

We define the initial state of walker+coin system as

$$|\phi_0\rangle = |\phi_0\rangle \otimes |\varphi_0\rangle, \tag{4}$$

where $|\varphi_0\rangle$ is the initial coin state. After N steps, the system evolves into

$$|\phi_N\rangle = [E(I_\mathrm{w} \otimes H)]^N |\phi_0\rangle. \tag{5}$$

The walker's phase distribution on a circle is

$$P(\theta) = \langle\theta|\rho_\mathrm{w}|\theta\rangle \tag{6}$$

with d being equally spaced values of $\theta = \theta_k$ and $\rho_\mathrm{w} = \mathrm{Tr_c}|\phi_N\rangle\langle\phi_N|$ is the reduced density matrix of the walker after tracing out the coin.

The standard deviation of the phase distribution, σ, which is the symbol of the spreading of the QW, is linear with respect to time t. Therefore, in sufficiently short time, the relation of phase spreading with time on a circle is a power law and satisfies[11]

$$\ln\sigma = \zeta \ln t + \xi, \tag{7}$$

where ζ is the slope coefficient and ξ is the intercept: $\zeta = 1$ for the QW and $\zeta = 1/2$ for the RW.

3. Physical implementation of QW

3.1. Quantum coin and walker

Circuit quantum electrodynamics (QED) is a device which is used to study the interaction between the quantum particle and the quantized electromagnetic mode inside a resonator. In this paper we consider a hybrid QED system of superconducting resonator-assisted quantum double-dot shown in Fig. 1(a). One of the dots, an electron that is shared by two adjacent dots coupled via tunneling, is capacitively coupled to the resonator. The double dots can be modeled as a double-well potential shown in Fig. 1(b). Generally, we apply an external magnetic field B_z of 100 mT along the axis z to the double dots.[45] Owing to the external magnetic field, there exists an energy difference between the two potentials and the electron can tunnel between the two quantum dots. We define the basis of qubits $|0\rangle$ for the electron appearing in the left dot and $|1\rangle$ for the electron in the right dot. From Fig. 1(b) we see the energy difference, namely the amount of energy consumption for moving the electron from the right dot to the left, between the states $|0\rangle$ and $|1\rangle$ is $\Delta = T$, where T is the rate of electron tunneling in the different dots.

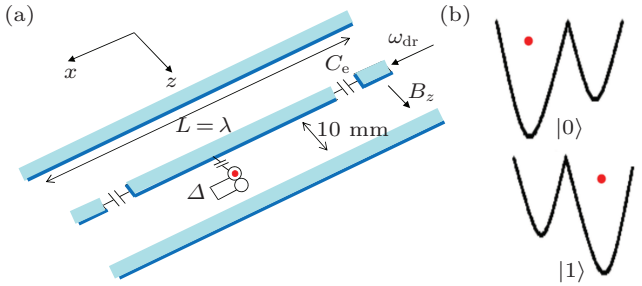


Fig. 1. (color online) (a) Experimental proposal for QW with superconducting resonator-assisted quantum double-dot. The red dot represents the electron. The coupling between the resonator and the double-dot can be switched on and off via an external electric field along the x axis. The superducting resonator is driven by a field along the x axis for implementing the coin flipping. (b) The double-dot modeled as a double-well potential. The basis of the qubit states represents the electron either in the left or right potential via tunneling. The energy difference between the states $|0\rangle$ and $|1\rangle$ is Δ.

After applying the magnetic field to the quantum dots, the double-well potential forms a circuit.[46] We just consider one circumstance, i.e., whether the electron is located in the left dot or right, the Hamiltonian describing the circuit is given by

$$\hat{H}_\mathrm{Q} = \sum_{N=0,1} E_\mathrm{c}(N - N_\mathrm{g})^2 |N\rangle\langle N| - \Delta\left(|N+1\rangle\langle N| + \mathrm{H.C.}\right), \tag{8}$$

where $E_\mathrm{c} = \mathrm{e}^2/2C_\mathrm{tot}$ is the charge energy, $C_\mathrm{tot} = C_\mathrm{g} + C_\mathrm{J}$ is the total capacitance in the circuit, C_J is the Josephson capacitance and C_g is voltage biased from a lead having capacitance to the circuit, $N_\mathrm{g} = C_\mathrm{g}V_\mathrm{g}/2e$ is the gate charge which represents the total polarization charge. Restricting the gate charge to the range $N_\mathrm{g} \in [0,1]$ by using the voltage V_g, the Hamiltonian in Eq. (8) is rewritten as

$$\hat{H}_\mathrm{Q} = \frac{1}{2}E_\mathrm{c}(1 - 2N_\mathrm{g})\sigma_z - \Delta\sigma_x. \tag{9}$$

So far, we have shown the Hamiltonian of the double-well potential. From Eq. (9) we see that the double-well potential presents the double-dot system with effective electric fields along the x and z directions, and the system with internal states $|0\rangle$ and $|1\rangle$ can be used as a two-level quantum coin.

Now we consider the circuit QED of double dots coupled to a superconducting resonator. The dots are located in the center of the resonator. If the oscillator mode of the resonator is coupled to the double-dot, by using the coordinate system transformation

$$R = \begin{pmatrix} \cos\theta & -\sin\theta \\ \sin\theta & \cos\theta \end{pmatrix},$$

and choosing $2N_\mathrm{g} = 1$, $\theta = \pi/2$, the Hamiltonian of the interacting qubit and resonator system with the rotating wave approximation takes the form ($\hbar = 1$)

$$\hat{H}_\mathrm{JC} = \omega_\mathrm{c} a^\dagger a + \frac{\Omega}{2}\sigma_z + g(a^\dagger\sigma_- + a\sigma_+), \tag{10}$$

where ω_c is the frequency of the resonator, and Ω[47] is the resonator-induced energy splitting of the qubit:

$$\Omega = \sqrt{E_c{}^2(1-2N_g)^2+4\Delta^2}$$

and

$$g = e\frac{C_g}{C_{tot}}\sqrt{\frac{\omega_c}{L}}$$

is the vacuum Rabi frequency. The form of Hamiltonian in Eq. (10) is the well-known Jaynes–Cummings (JC) model.[48]

3.2. Coin flipping and conditional phase shift operator

In our hybrid system, the walker can be represented by the phase state of the single mode of the resonator and the coin is the two-level energy system. To implement the coin flipping operator, a microwave time-dependent driving field is applied to the circuit QED system with the form

$$\hat{H}_d = \varepsilon(t)(a^\dagger e^{-i\omega_d t} + a e^{i\omega_d t}), \tag{11}$$

where ω_d is the frequency of driving field. Let $\varepsilon(t)$ be a square wave, so ε is a constant when the field is turned on, while if it is zero, then the field is off. The Hamiltonian of the hybrid system, containing the driving field, is

$$\hat{H}_{tot} = \hat{H}_{JC} + \hat{H}_d. \tag{12}$$

In the dispersive regime,

$$|\delta| = |\Omega - \omega_c| \gg g. \tag{13}$$

To calculate the effective Hamiltonian from Eq. (12), we introduce the unitary transformation $\hat{S} = \exp[g/\delta(a\sigma_+ - a^\dagger\sigma_-)]$, and use the translation equation $\hat{S}^\dagger\hat{H}_{tot}\hat{S}$,[46,49] the Hamiltonian in Eq. (12) turns into the effective Hamiltonian of the whole system with driving field

$$\hat{H}_{eff} = \chi a^\dagger a\sigma_z - \frac{1}{2}\delta_1\sigma_z - \delta_2 a^\dagger a + \frac{1}{2}\Omega_2\sigma_x + \varepsilon(a^\dagger + a), \tag{14}$$

with $\delta_1 = \omega_d - \Omega$, $\delta_2 = \omega_d - \omega_c$, $\Omega_2 = 2g\varepsilon/\delta_2$, and $\chi = g^2/\delta$.

The free evolution

$$\exp(-i\hat{H}_{eff}t) \tag{15}$$

continues even when the driving field is off ($\varepsilon = 0$).

By choosing the coherent state $|\alpha = 3\rangle$ and different values of ε, we show the probability distribution of the walker in PS at the 4th step with step size $\Delta\theta = 0.3$ (Fig. 2). The solid line represents the circumstance with $\varepsilon = 0.01$ GHz, whereas the dashed line represents the circumstance with $\varepsilon = 0.012$ GHz. From Fig. 2 we see that the peak probability with $\varepsilon = 0.012$ GHz is smaller than that with $\varepsilon = 0.01$ GHz because the evolution of the last term in Eq. (14) provides a displacement operator in position space and pushes the walker off the circle in PS. Apart from this, the rate of probability on the position $\theta = 0.01$ GHz in the three main peaks with $\varepsilon = 0.012$ GHz is higher than that with $\varepsilon = 0.01$ GHz, that is to say, the decoherence drives the probability to the origin position, making the distribution be Gaussian distribution. These can be regarded as the decoherence on the walker in PS and with decoherence increasing we can observe the QW–RW transmission.

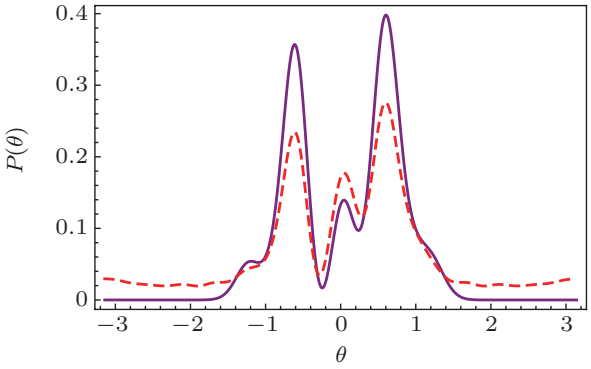


Fig. 2. (color online) The probability distributions of the walker in PS at the 4th step with the initial walker state $|\alpha = 3\rangle$ and coin state $(|0\rangle + i|1\rangle)/\sqrt{2}$, the step size $\Delta\theta = 0.3$, and $\varepsilon = 0.01$ GHz in solid line and $\varepsilon = 0.012$ GHz in dashed line respectively. The phase distribution shows a ballistic behavior of the QW in PS. With the strength of the driving field increasing, the decoherence introduced by displacement in position space increases and the phase distribution tends to be the combination of those of QW and RW.

The evolution of the hybrid system is described by the effective Hamiltonian. The first term on the right-hand side in Eq. (14) contains $a^\dagger a\sigma_z$, which proves an interrelated relationship between the walker and coin, and makes the walker evolve along clockwise or counterclockwise at the same constant angle with the orientation based on the state of the coin. The second and third terms involve the operators σ_z and $a^\dagger a$, which represent the consequent frequency of walker and the energies for the coin, respectively. The fourth term contains σ_x and it can translate into the Hadamard coin flip by choosing a suitable pulse time. The coefficient is proportional to the Rabi frequency. The last term is the displacement in the position space and pushes the walker off the circle in PS. Thus it also causes the decoherence in the QW in PS.

4. Numerical analysis

Now all the factors that the implementation of QW needs are fulfilled. To make the scheme work, the value of constant coefficient ε in the last term in Eq. (14) which brings the displacement in PS must be kept very small. Nevertheless, the Rabi frequency Ω_2 is proportional to the pulsed driving field ε, so, no matter how small the value of ε is, we can choose a suitable pulse time to transform the σ_x into Hadamard coin flip.

We choose the initial coin state as

$$|\varphi_0\rangle = (|0\rangle + i|1\rangle)/\sqrt{2}, \tag{16}$$

set the initial field in the resonator as coherent state

$$|\alpha\rangle = \exp\left(-\frac{|\alpha|^2}{2}\right)\sum\frac{\alpha^n}{\sqrt{n!}}|n\rangle, \tag{17}$$

and obtain the realistic system parameters as follows:[50,51]

$$(\Omega,\omega_c,g)/2\pi = (0.7,0.5,0.01)\ \text{GHz}. \tag{18}$$

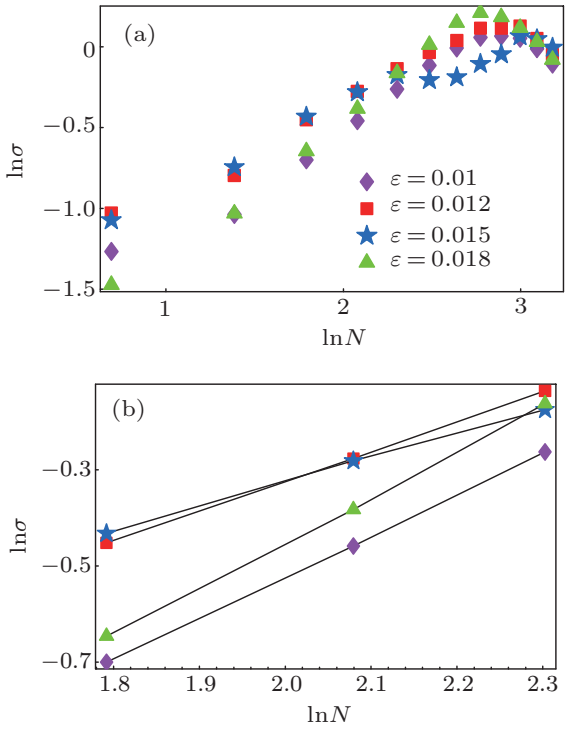


Fig. 3. (color online) (a) The ln–ln plots of the standard deviation of the phase distribution σ versus step number N with the initial walker state $|\alpha = 3\rangle$, coin state $(|0\rangle + \mathrm{i}|1\rangle)/\sqrt{2}$ and different field strengths with $\varepsilon = (0.01, 0.012, 0.015, 0.018)$ GHz, the step size in PS $\Delta\theta = 0.3$. The dots represent the standard deviation of even steps up to 25 steps. (b) The ln–ln plots with various ε values showing the slopes of the plots which represent the values of the walker spreading speed ς.

In Fig. 3(a), we show the ln–ln plots of the standard deviation of the probability distribution of the walker in PS with step size $\Delta\theta = 0.3$ only even steps without losing generality, the diamonds, squares, stars, triangles represent the standard deviations of the phase distribution of QW in PS with different $\varepsilon = (0.01, 0.012, 0.015, 0.018)$ GHz, respectively. With the step number increasing, the wave function of the walker meets itself on the circle in PS after 15 steps. Thus after 15 steps, the curve of the ln–ln plot of standard deviation versus the step number drops down. This shows the difference from the QW on the line, though for the first few steps QWs on both circle and line show the ballistic behavior as expected. Overall, the slope of the points becomes small with increasing constant ε. To realize the scenario more intuitively, we cut out the standard deviation after 6, 8, and 10 steps and connect the points into a line of the whole circumstance (Fig. 3(b)). The figure shows the slopes of the line ς which correspond to the diamonds, squares, stars, triangles are about 1, 0.89, 0.64, 0.53 respectively. Using Eq. (7) as a reference, the slopes are 1 for QW and 0.5 for RW respectively, different slopes of the ln–ln plots show the different behaviors of the walker on the circle in PS with different levels of decoherence. The decoherence is introduced by the driving field which leads the walker to move in position space too. For QW in PS, it is equivalent to decoherence. With the strength of the driving field increasing the decoherence increases. Hence with decoherence increasing we see the QW–RW transition. With increasing the value of ε, the trend QW changes to RW is more obvious. So, in order to keep the more prominent properties of QW, ε must be small enough.

5. Conclusions

We show how a QW in PS can be implemented in a quantum quincunx created through superconducting resonator-assisted quantum double dots and how interpolation from a quantum to a random walk is implemented by controllable decoherence introduced by the displacement of the walker in position space. Our scheme shows how a QW with just one walker can be implemented in a realistic system. The coin flipping operation is implemented by driving the resonator directly, and at the same time the driving field also introduces the displacement of the walker in position space and pushes the walker off the circle in PS. Thus the displacement in position space is equivalent to decoherence on the walker in PS which is controlled by the strength of the driving field. With the strength of the driving field increasing the decoherence increases and we observe the QW–RW transition.

Although in our paper we make use of the decoherence introduced by the driving field to show the transition from QW to RW, which is one of the main points of our paper, for most of the applications of QW it requires quadratic enhancement of walker spreading. The decoherence induced by the driving field can be compensated for by the method in Ref. [11]. The displacement of the walker in position space pushes the walker off the circle in PS by changing the mean photon number of the resonator field. Hence we can adjust the pulse duration each time t_i according to the predicted mean photon number $\bar{n}(i)$, that is, $t_i = [\delta + 2\bar{n}(i) - 2g\varepsilon/\delta]\pi/4g\varepsilon$, to compensate for the effect due to the displacement and obtain a perfect QW in PS.

References

[1] Aharonov Y, Davidovich L and Zagury N 1993 *Phys. Rev. A* **48** 1687
[2] Ambainis A 2003 *Int. J. Quantum Inform.* **1** 507
[3] Childs A M, Cleve R, Deotto E, Farhi E, Gutmann S and Spielman D A 2003 *Proc. 35th ACM Symposium on Theory of Computing (STOC 2003)* pp. 59–68
[4] Shenvi N, Kempe J and Whaley K B 2003 *Phys. Rev. A* **67** 052307
[5] Zhang R, Xu Y and Xue P 2015 *Chin. Phys. B* **24** 010303
[6] Zhang R, Xue P and Twamley J 2014 *Phys. Rev. A* **89** 042317

[7] Zhang R and Xue P 2014 *Quantum Information Processing* **13** 1825
[8] Zhang R, Qin H, Tang B and Xue P 2013 *Chin. Phys. B* **22** 110312
[9] Brun T A, Carteret H A and Ambainis A 2003 *Phys. Rev. Lett.* **91** 130602
[10] Xue P and Sanders B C 2008 *New J. Phys.* **8** 053025
[11] Xue P, Sanders B C, Blais A and Lalumiére K 2008 *Phys. Rev. A* **78** 042334
[12] Hardal A C, Xue P, Shikano Y, Müstecaploğlu Ö E and Sanders B C 2013 *Phys. Rev. A* **88** 022303
[13] Zähringer F, Kirchmair G, Gerritsma R, Solano E, Blatt R and Roos C F 2010 *Phys. Rev. Lett.* **104** 100503
[14] Schmitz H, Matjeschk R, Schneider Ch, Glueckert J, Enderlein M, Huber T and Schaetz T 2009 *Phys. Rev. Lett.* **103** 090504
[15] Xue P, Sanders B C and Leibfreid D 2009 *Phys. Rev. Lett.* **103** 183602
[16] Bouwmeester D, Marzoli I, Karman G P, Schleich W and Woerdman J P 1999 *Phys. Rev. A* **61** 013410
[17] Do B, Stohler M L, Balasubramanian S, Elliott D S, Eash C, Fischbach E, Fischbach M A, Mills A and Zwickl B 2005 *J. Opt. Soc. Am. B* **22** 499
[18] Zhang P, Ren X F, Zou X B, Liu B H, Huang Y F and Guo G C 2007 *Phys. Rev. A* **75** 052310
[19] Peruzzo A, Lobino M, Matthews J C F, Matsuda N, Politi A, Poulios K, Zhou X, Lahini Y, Ismail N, Wörhoff K, Bromberg Y, Silberberg Y, Thompson M G and O'Brien J L 2010 *Science* **329** 1500
[20] Perets H B, Lahini Y, Pozzi F, Sorel M, Morandotti R and Silberberg Y 2008 *Phys. Rev. Lett.* **100** 170506
[21] Sansoni L, Sciarrino F, Vallone G, Mataloni P, Crespi A, Ramponi R and Osellame R 2012 *Phys. Rev. Lett.* **108** 010502
[22] Jeong Y C, Franco C Di, Lim H T, Kim M S and Kim Y H 2013 *Nat. Commun.* **4** 2471
[23] Broome M A, Fedrizzi A, Lanyon B P, Kassal I, Aspuru-Guzik A and White A G 2010 *Phys. Rev. Lett.* **104** 153602
[24] Xue P, Qin H, Tang B and Sanders B C 2014 *New J. Phys.* **16** 053009
[25] Schreiber A, Cassemiro K N, Potoček V, Gábris A, Mosley P J, Andersson E, Jex I and Silberhorn C 2012 *Science* **336** 55
[26] Xue P, Qin H and Tang B 2014 *Sci. Rep.* **4** 4825
[27] Xue P, Qin H, Tang B, Zhan X, Bian Z H and Li J 2014 *Chin. Phys. B* **23** 110307
[28] Bian Z H, Li J, Qin H, Zhan X, Zhang R, Sanders B C and Xue P 2015 *Phys. Rev. Lett.* **114** 203602
[29] Chen H W, Kong X, Chong B, Qin G, Zhou X Y, Peng X H and Du J F 2011 *Phys. Rev. A* **83** 032314
[30] Kuznetsova M S, Flisinski K, Gerlovin I Ya, Petrov M Yu, Ignatiev I V, Verbin S Yu, Yakovlev D R, Reuter D, Wieck A D and Bayer M 2014 *Phys. Rev. B* **89** 125304
[31] Culcer D, Saraiva A L, Koiller B, Hu X D and Sarma S D 2012 *Phys. Rev. Lett.* **108** 126804
[32] Paudel H P and Leuenberger M N 2013 *Phys. Rev. B* **88** 085316
[33] Petta J R, Johnson A C, Taylor J M, Laird E A, Yacoby A, Lukin M D, Marcus C M, Hanson M P and Gossard A C 2005 *Science* **309** 2180
[34] Johnson A C, Petta J R, Taylor J M, Yacoby A, Lukin M D, Marcus C M, Hanson M P and Gossard A C 2005 *Nature* **435** 925
[35] Solenov D, Economou S E and Reinecke T L 2013 *Phys. Rev. B* **87** 035308
[36] Burkard G and Imamoglu A 2006 *Phys. Rev. B* **74** 041307
[37] Lin Z R, Guo G P, Tu T, Zhu F Y and Guo G C 2008 *Phys. Rev. Lett.* **101** 230501
[38] Golovach V N, Borhani M and Loss D 2010 *Phys. Rev. A* **81** 022315
[39] Burda Z, Duda J, Luck J M and Waclaw B 2009 *Phys. Rev. Lett.* **102** 160602
[40] Xue P 2013 *J. Comput. Theor. Nanosc.* **10** 1
[41] Tang B, Qin H, Zhang R, Liu J M and Xue P 2014 *Chin. Phys. B* **23** 050307
[42] Xue P 2010 *Phys. Lett. A* **374** 2601
[43] Xue P and Sanders B C 2013 *Phys. Rev. A* **87** 022334
[44] Sanders B C, Bartlett S D, Tregenna B and Knight P L 2003 *Phys. Rev. A* **67** 042305
[45] Taylor J M, Engel H A, Dür W, Yacoby A, Marcus C M, Zoller P and Lukin M D 2005 *Nat. Phys.* **1** 177
[46] Blais A, Huang R S, Wallra A, Girvin S M and Schoelkopf R J 2004 *Phys. Rev. A* **69** 062320
[47] Schoelkopf R, Clerk A, Girvin S, Lehnert K and Devoret M 2003 *Quantum Noise in Mesoscopic Physics* (Dordrecht: Kluwer Academic) Chap. 9, pp. 175–203
[48] Jaynes E T and Cummings F W 1963 *Proc. IEEE* **51** 89
[49] James D F and Jerke J 2007 *Can. J. Phys.* **85** 625
[50] Schuster D I, Houck A A, Schreier J A, Wallraff A, Gambetta J M, Blais A, Frunzio L, Majer J, Johnson B, Devoret M H, Girvin S M and Schoelkopf R J 2007 *Nature* **445** 515
[51] Blais A, Gambetta J, Wallraff A, Schuster D I, Girvin S M, Devoret M H and Schoelkopf R J 2007 *Phys. Rev. A* **75** 032329